

STIMULUS-INDUCED SYNCHRONIZATION  
IN HODGKIN–HUXLEY-TYPE MODEL NEURONS  
OF CAT RETINAL GANGLION CELLS\*

M.K.N. AFGHAN, P. JUNG, A. NEIMAN, M. ROWE

Quantitative Biology Institute, Ohio University  
Athens, Ohio 45701, USA

*(Received February 21, 2006)*

Visual signals converge through the layers of the retinal circuitry from the photoreceptor cells to the retinal ganglion cells such that nearby ganglion cells are driven by essentially the same visual stimulus. We use computational modeling to address the question whether the experimentally observed degree of synchrony in nearby ganglion cells is due to the common visual stimulus or whether active network circuitry is necessary.

PACS numbers: 89.19.La, 87.17.Nn, 05.45.-a, 05.40.Ca

## 1. Introduction

Visual signals are received by the photoreceptor cells, where they are converted into electrical signals. The photoreceptor cells contact horizontal cells that form a sheet of cells where inhibition spreads laterally to nearby photoreceptor cells in response to visual stimuli. The spatial spread of the visual signal generates stimuli to the bipolar cells that originate from a large number of photoreceptor cells, described by a receptive field. The convergence of the visual signal continues downstream as a number of bipolar cells, with similar inputs, output to the retinal ganglion cells and thus provide almost identical input to two nearby retinal ganglion cells. A number of studies in a variety of species have reported that these cells show spike synchronization in their stimulus-induced responses [1–3]. This synchronization exhibits various time scales and its role in visual information processing is an unresolved issue of brain research. In this paper we study synchronization in two retinal ganglion cells that are driven by the same visual stimulus using computational modeling.

---

\* Presented at the XVIII Marian Smoluchowski Symposium on Statistical Physics, Zakopane, Poland, September 3–6, 2005.

## 2. Methods

Based on an earlier work on tiger salamander retina a Hodgkin–Huxley type neuron model has been put forward for the cat retinal ganglion cells [4, 5]. Their model included four voltage-gated currents:  $\text{Na}^+$  current ( $I_{\text{Na}}$ ),  $\text{Ca}^{2+}$  current ( $I_{\text{Ca}}$ ), delayed rectifier (non-inactivating)  $\text{K}^+$  current ( $I_{\text{K}}$ ), A-type (inactivating)  $\text{K}^+$  current ( $I_{\text{A}}$ ), and one  $\text{Ca}^{2+}$ -activated  $\text{K}^+$  current ( $I_{\text{KCa}}$ ). In order to account for spontaneous activity, the equation for the voltage is modified by including zero-mean, Gaussian white noise  $\xi(t)$  that mimics synaptic noise. Furthermore, a nonspecific, voltage-independent leak current,  $I_{\text{L}}$ , is included in our model. The equation for the membrane potential  $V$  (in units of mV) reads

$$C \left( \frac{dV}{dt} \right) = -(I_{\text{Na}} + I_{\text{K}} + I_{\text{Ca}} + I_{\text{A}} + I_{\text{KCa}} + I_{\text{L}}) - I(t) + \xi(t), \quad (1)$$

where  $C = 1\mu\text{F}/\text{cm}^2$  denotes the specific membrane capacitance,  $I(t)$  is the injected current density to the cell, and  $\langle \xi(t)\xi(t') \rangle = 2\epsilon\delta(t-t')$  with the noise strength  $\epsilon$ . The ionic currents densities are given by  $I_{\text{Na}} = \bar{g}_{\text{Na}}hm^3(V - V_{\text{Na}})$ ,  $I_{\text{K}} = \bar{g}_{\text{K}}n^4(V - V_{\text{K}})$ ,  $I_{\text{Ca}} = \bar{g}_{\text{Ca}}c^3(V - V_{\text{Ca}})$ ,  $I_{\text{A}} = \bar{g}_{\text{A}}a^3h_{\text{A}}(V - V_{\text{K}})$ ,  $I_{\text{KCa}} = g_{\text{KCa}}(V - V_{\text{K}})$ ,  $I_{\text{L}} = g_{\text{L}}(V - V_{\text{L}})$ , where  $\bar{g}_j$  are the maximal conductances, *i.e.*  $\bar{g}_{\text{Na}} = 60$ ,  $\bar{g}_{\text{Ca}} = 2.0$ ,  $\bar{g}_{\text{K}} = 12.0$ ,  $\bar{g}_{\text{A}} = 36.0$ ,  $g_{\text{L}} = 0.2$  in units of  $\text{mS}/\text{cm}^2$ , and  $V_j$  the reversal potentials, *i.e.*  $V_{\text{Na}} = 35$  mV,  $V_{\text{K}} = -75.0$  mV,  $V_{\text{L}} = -60.0$  V and  $\epsilon = 5.0\mu\text{A}^2/\text{cm}^2$ . The noise strength  $\epsilon$  has been adjusted to account for the experimentally observed spontaneous spiking rate of about 25/s under *dark* conditions. The quantity  $g_{\text{KCa}}$  denotes the calcium-dependent potassium conductance,  $g_{\text{KCa}} = \bar{g}_{\text{KCa}}[\text{Ca}]_i^2/(1 + [\text{Ca}]_i^2)$ , where  $\bar{g}_{\text{KCa}} = 0.05\text{mS}/\text{cm}^2$ . Here  $[\text{Ca}^{2+}]_i$  denotes intracellular calcium concentration, and  $\bar{g}_{\text{KCa}}$  the maximal conductance. The reversal potentials for all ionic currents except for  $\text{Ca}^{2+}$  were kept fixed since for the small capacitance the change in ionic intracellular and extracellular concentration is small. The reversal potential for  $\text{Ca}^{2+}$ ,  $V_{\text{Ca}}$ , was updated dynamically according to the Nernst equation with the intracellular calcium concentration governed by [4, 5]

$$\frac{d[\text{Ca}^{2+}]_i}{dt} = -0.000015I_{\text{Ca}} - 0.02([\text{Ca}^{2+}]_i - 0.0001). \quad (2)$$

The gating variables ( $m$ ,  $h$ ,  $c$ ,  $n$ ,  $a$ , and  $h_{\text{A}}$ ) satisfy first order kinetics with the opening and closing rates

$$\alpha_m = \frac{-0.05(V + 30)}{\exp(-0.1(V + 30)) - 1}, \quad \beta_m = 0.5 \exp\left(-\frac{V + 55}{18}\right),$$

$$\begin{aligned}
 \alpha_h &= 0.0182 \exp\left(-\frac{V+50}{20}\right), & \beta_h &= \frac{0.35}{\exp(-0.1(V+20)) + 1}, \\
 \alpha_n &= \frac{-0.004(V+40)}{\exp(-0.1(V+40)) - 1}, & \beta_n &= 0.025 \exp\left(-\frac{V+50}{80}\right), \\
 \alpha_c &= \frac{-0.003(V+13)}{\exp(-0.1(V+13)) - 1}, & \beta_c &= 0.0467 \exp\left(-\frac{V+38}{18}\right), \\
 \alpha_A &= \frac{-0.0011(V+90)}{\exp(-0.1(V+90)) - 1}, & \beta_A &= 6.6710^{-3} \exp\left(-\frac{V+30}{10}\right), \\
 \alpha_{h_A} &= 0.105 \exp\left(-\frac{V+70}{20}\right), & \beta_{h_A} &= \frac{0.1}{\exp(-0.1(V+40)) + 1}. \tag{3}
 \end{aligned}$$

Numerical integration of Eq. (1), referred to as the model hereafter, has been performed using a first order stochastic solver with integration time step  $\Delta t = 10^{-5}$ . The firing threshold to detect action potentials was set at  $-20$  mV, and the spikes times  $\{t_i\}$  were recorded every time membrane potential crossed firing threshold with positive slope.

To mimic visual input  $I(t)$  to the ganglion cells the model neurons are driven with stimulus of the form  $I(t) = I_0 + y(t)$ , where  $I_0$  is a constant background current and  $y(t)$  denotes Gaussian, exponentially correlated noise with correlation time  $\tau$  (in ms) and variance  $D$  (in  $\mu A^2/cm^4$ ). The stationary correlation function  $K(t - t')$  and power spectrum  $S(\omega)$  of  $y(t)$  are given by

$$K(t - t') = D \exp\left(\frac{-|t - t'|}{\tau}\right), \quad S(\omega) = \frac{2D\tau}{(1 + \omega^2\tau^2)}. \tag{4}$$

The power spectrum decays proportional to  $\omega^{-2}$  for  $\omega \gg 1/\tau$ . Hence  $1/\tau$  characterizes the frequency content of the visual signal  $y(t)$ . The total power, *i.e.* the integral over the power spectrum is given by  $2\pi D$  and is independent of  $\tau$ . The white noise limit  $\tau \rightarrow 0$  at fixed finite variance  $D$  is thus characterized by a uniform power spectrum with amplitude approaching zero everywhere. In the limit  $\tau \rightarrow \infty$  the power becomes concentrated at low-frequencies generating slow random changes with finite variance.

The instantaneous phase  $\Phi(t)$  is defined as (for a detailed discussion see in [6])

$$\Phi(t) = 2\pi i + 2\pi \frac{(t - t_i)}{(t_{i+1} - t_i)}, \quad t_i \leq t < t_{i+1}, \tag{5}$$

where  $t_i$  denote the times at which action potentials occur. The phase increases by  $2\pi$  every time the neuron fires. In between two subsequent firing events at times  $t_i$  and  $t_{i+1}$  the phase is determined by linear interpolation between the phases at times  $t_i + \varepsilon$  and  $t_{i+1} - \varepsilon$ .

The probability density  $P(\phi)$  of the phase difference  $\Phi_1(t) - \Phi_2(t)$  collapsed to the interval  $[0, 2\pi]$  is the simplest measure of synchronization. In the case of perfect synchronization  $P(\phi)$  is given by a  $\delta$ -function,  $P(\phi) = \delta(\phi - \phi_0)$ , where  $\phi_0$  is a constant phase shift. In the opposite limit of no synchronization, the probability density  $P(\phi)$  is uniform. Between these limiting cases the existence of a well expressed peak in the  $P(\phi)$  signifies stochastic synchronization. The existence of this peak can be characterized by single numbers, called synchronization indices. We use here two indices. First is the intensity of the first Fourier mode of the probability density  $P(\phi)$  calculated as [6]

$$\gamma^2 = \langle \cos \phi(t) \rangle^2 + \langle \sin \phi(t) \rangle^2, \quad (6)$$

where  $\langle \dots \rangle$  denotes temporal averaging. The index  $\gamma$  assumes values between 0 (no synchronization) and 1 (perfect phase locking for noise free case). The second index is based on the Shannon entropy of  $P(\phi)$  normalized to its maximal value for the uniform distribution,  $S_{\max} = \ln(2\pi)$  [6], *i.e.*

$$\rho = \frac{S_{\max} - S}{S_{\max}}, \quad \text{where} \quad S = - \int_0^{2\pi} P(\phi) \ln P(\phi) d\phi. \quad (7)$$

### 3. Results

First we consider the bifurcations in the deterministic model. We used the AUTO software package to perform the bifurcation analysis of the model. Fig. 1 shows the bifurcation diagram of the model for the bifurcation parameter  $I(t) = I_{dc}$ . The system exhibits saddle-node bifurcations at SN1, SN2 and SN3 for the approximate bifurcation parameter values of  $0.2517 \mu\text{A}/\text{cm}^2$ ,  $0.2515 \mu\text{A}/\text{cm}^2$  and  $0.2501 \mu\text{A}/\text{cm}^2$ , respectively. A pair of stable and unstable periodic orbits are bifurcated through the saddle-node bifurcation of periodic orbits at point SN3. The unstable part vanishes through a subcritical Hopf bifurcation at point HB1 for  $I_{dc} \approx 0.622 \mu\text{A}/\text{cm}^2$  making the fixed point unstable. At point HB2, the system undergoes a supercritical Hopf bifurcation and the fixed point loses its stability giving birth to a stable periodic orbit.

Next we study the firing characteristics of the excitable model neuron when stimulated with the random visual signal  $y(t)$  in terms of the firing rate and coefficient of variation (CV), *i.e.* the ratio of the variance of the interspike intervals and the mean interspike interval. For the rest of the discussion, the background current  $I_0$  and synaptic noise intensity are kept fixed at  $0.15 \mu\text{A}/\text{cm}^2$  and  $5.0 \mu\text{A}^2/\text{cm}^4$ , respectively. Fig. 2(a) shows the firing rate whereas Fig. 2(b) shows the CV as a function of the correlation time  $\tau$  of the visual stimulus. In the limit  $\tau \rightarrow 0$ , the power spectrum of the visual

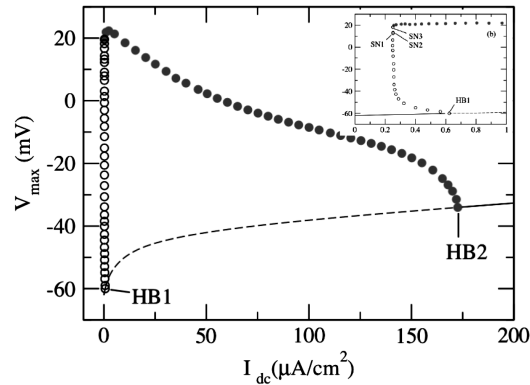


Fig. 1. Bifurcation diagram: The maximal value of the membrane potential as a function of bifurcation parameter  $I_{dc}$  is shown. Solid (dotted) line denotes stable (unstable) fixed points whereas filled (empty) circles denote stable (unstable) periodic orbits. SN and HB denote saddle-node and Hopf bifurcations, respectively. The inset shows an enlarged section.

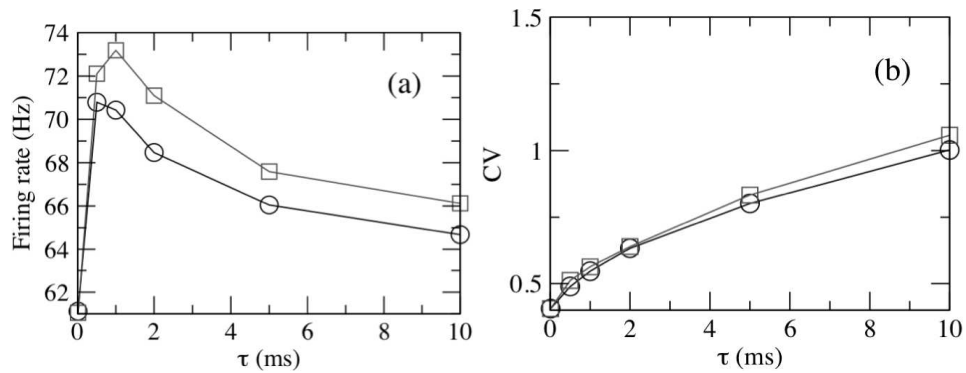


Fig. 2. Firing rate (a) and CV (b) as a function of correlation time  $\tau$ , of the visual signal  $y(t)$  for  $D = 30 \mu A^2/cm^4$  (circles) and  $D = 40 \mu A^2/cm^4$  (squares).

signal  $y(t)$  (see Eq. (4)) becomes flat with *vanishing* amplitude — hence the firing rate is solely determined by synaptic noise  $\xi(t)$ . For increasing  $\tau$ , the firing rate reaches a maximum and then decreases to zero for  $\tau \rightarrow \infty$  since  $y(t)$  slowly modulates the excitation threshold giving rise to infinitely long periods of large thresholds during which the synaptic noise cannot generate action potentials. The firing rate increases and the maximum shifts to larger  $\tau$  for increasing  $D$ . The monotonously increasing CV indicates that the firing becomes more irregular as the correlation time  $\tau$  is increased and hence that the maximum of the firing rate is not due to a dynamic resonance.

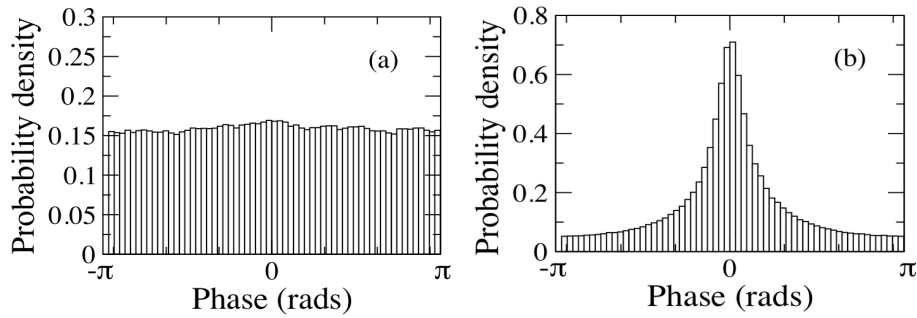


Fig. 3. Probability densities of phase difference of two non-coupled model neurons, stimulated with common visual noise at  $D = 30\mu\text{A}^2/\text{cm}^4$  for  $\tau = 0.01$  ms (a) and  $\tau = 2$  ms (b).

To investigate synchronization in two model cells caused by common random visual stimuli with varying frequency contents, we stimulate two non-coupled neurons with the same visual random input  $y(t)$ . Both neurons are in excitable regime which is different from the studies on synchronization of limit cycle oscillators by common noise [7, 8]. For the small correlation time  $\tau = 0.01\text{ms}$  the probability density of the phase differences is almost uniform as shown in Fig. 3(a), indicating a small degree of synchronization. For  $\tau = 2\text{ms}$ , a pronounced peak can be seen in the probability density (Fig. 3(b)) indicating a preferred value of the phase difference. The two synchronization indices are plotted in Fig. 4 as a function of the correlation time  $\tau$  of the common visual input signal  $y(t)$ . The two non-coupled cells show almost no synchronization for small correlation times. But as the

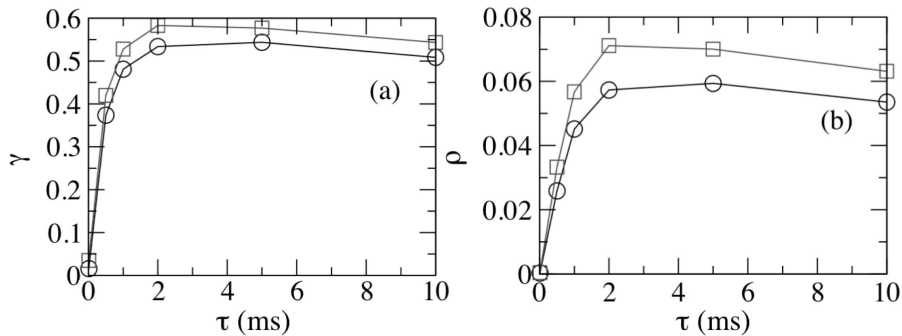


Fig. 4. Synchronization indices for two non-coupled model neurons *versus* cut-off frequency when stimulated with common visual noise with  $D = 30\mu\text{A}^2/\text{cm}^4$  (circles) and  $D = 40\mu\text{A}^2/\text{cm}^4$  (squares).

correlation time increases the degree of synchrony of the firing of the two cells increases, approaches a maximum and then decreases to zero. The maximum synchrony appears at  $\tau = 2$  ms, independent of the noise variance. Since the correlation time  $\tau$  determines the frequency content of the visual signal, our findings above indicate that stimulus-induced synchrony in the visual system can occur for selective visual signals with proper frequency content.

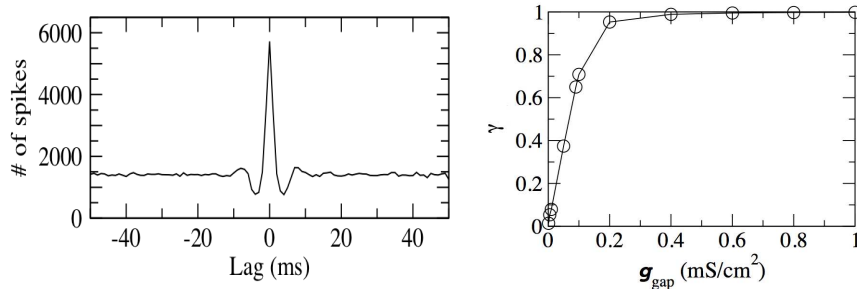


Fig. 5. Left panel: Cross-correlation histogram for two non-coupled model cells, stimulated with colored visual noise with  $D = 30\mu\text{A}^2/\text{cm}^4$  and  $\tau = 2$  ms. Right panel: Synchronization index for two model cells coupled through gap junction versus gap junction conductance.

Typically, interactions between pairs of neurons are assessed by constructing cross-correlation histograms (CCH) [9,10], which quantify the relative timing of spikes in one spike train with respect to a second spike train. A sharp peak around zero delay in CCH reflects spike synchronization between the two cells, and the width of the peak serves as a measure of the time scale of these interactions. Let us consider the CCH for a case where the two non-coupled model cells are stimulated with the common visual noise  $y(t)$  of variance  $D = 30\mu\text{A}^2/\text{cm}^4$  and correlation time  $\tau = 2$  ms. The narrow peak in Fig. 5 represents precise synchronization within a few ms. The synchronization index in this case is  $\gamma = 0.53$ . Such a CCH is similar to a typical experimental CCH.

The standard deviation of the input signal to produce such a tight synchrony is in the range of currents received typically by the ganglion cells ( $5\text{--}10 \mu\text{A}/\text{cm}^2$ ) [11], corresponding to a rather strong stimulation. However, weak stimuli, which are physiologically interesting, fail to synchronize uncoupled noisy cells. In particular, when the model cells are driven with the common visual noise  $y(t)$  with a standard deviation of  $\leq 0.5\mu\text{A}/\text{cm}^2$ , their responses show no synchronization (data not shown). Thus, common weak random stimuli fail to account for the tight synchrony and thus additional

mechanisms should be employed to enable weak stimulus synchronization. One possibility is to use gap junctions as suggested by many experimental studies [3, 12, 13]. We thus couple the model cells through a gap junction, that is a term  $I_{\text{gap}} = g_{\text{gap}}(V - V_{\text{pre}})$ , where  $g_{\text{gap}}$  is the gap junction conductance and  $V_{\text{pre}}$  is the presynaptic membrane potential, is added to Eq. (1) of the model. The dependence of the synchronization index  $\gamma$  on the gap junction conductance  $g_{\text{gap}}$ , when the two coupled model cells are stimulated with weak visual noise of variance  $D = 0.25\mu\text{A}^2/\text{cm}^4$  and correlation time  $\tau = 2$  ms, is shown in the right panel of Fig. 5. For  $g_{\text{gap}} \geq 0.4$  mS/cm<sup>2</sup>, the cells exhibit almost perfect synchronization. From the right panel of Fig. 5 it is clear that in order to obtain synchronization for the pair of model cells with an index of  $\gamma = 0.53$  which corresponds to a typical experimental CCH gap junction conductance of  $g_{\text{gap}} \approx 0.08$  mS/cm<sup>2</sup> is required.

#### 4. Summary

In this work, we investigated synchronization of cat retinal ganglion cells facilitated by common visual stimulus with variable frequency content. We find that the model cells optimally synchronize for input signals with appropriate strength and frequency content. Other studies have shown resonance-type dependence of the information gain [14] and of the spike time reliability [15] on the frequency content of noisy stimuli. Our study suggests that for weak stimuli tight spike synchrony requires coupling of model cells through gap junction with an estimated 0.08 mS/cm<sup>2</sup> gap junction conductance.

#### REFERENCES

- [1] D. Arnett, T. Spraker, *J. Physiol.* **317**, 29 (1981).
- [2] J. Jonsen, M. Levine, *J. Physiol.* **345**, 439 (1983).
- [3] D. Mastrorarde, *J. Neurophysiol.* **49**, 303 (1983); *J. Neurophysiol.* **49**, 325 (1983); *J. Neurophysiol.* **49**, 350 (1983).
- [4] J. Fohlmeister, P. Coleman, R. Miller, *Brain Res.* **510**, 343 (1990).
- [5] A. Przybyszewski, M. Lankert, W. van de Grind, *Biol. Cybern.* **74**, 299 (1996).
- [6] M. Rosenblum, A. Pikovsky, J. Kurths, C. Schäfer, P. Tass, *Handbook of Biological Physics*, vol. 4, Elsevier, Amsterdam 2001, pp. 279-321.
- [7] R. Jensen, L. Jones, D. Gartner, *Computational Neuroscience: Trends in Research*, Ed. J. Bower, Plenum, New York 1998, pp. 403-407.
- [8] D. Goldobin, A. Pikovsky, *Phys. Rev.* **E71**, 045201 (2005).
- [9] D. Mastrorarde, *Trends in Neuroscience* **12**, 75 (1989).
- [10] A. Sillito, H. Jones, G. Gerstein, D. West, *Nature* **369**, 479 (1994).

- [11] M.A. Freed, *J. Neurophysiol.* **83**, 2956 (2000).
- [12] S.H. De Vries, *J. Neurophysiol.* **81**, 908 (1999).
- [13] E. Hu, S. Bloomfield, *J. Neurosci.* **23**, 6768 (2003).
- [14] M.J. Chacron, A. Longtin, L. Maler, *J. Neurosci.* **21**, 5328 (2001).
- [15] J.D. Hunter, J.G. Milton, P.J. Thomas, J.D. Cowan, *J. Neurophysiol.* **80**, 1427 (1998).